Numerical modelling of depositional sequences in half-graben rift basins

ROB L. GAWTHORPE, STUART HARDY and BRYAN RITCHIE[1]
Basin and Stratigraphic Studies Group, Department of Earth Sciences, University of Manchester, Manchester M13 9PL, UK (E-mail: Rob.Gawthorpe@man.ac.uk)

ABSTRACT

A three-dimensional numerical model of sediment transport and deposition in coarse-grained deltas is used to investigate the controls on depositional sequence variability in marine half-graben extensional basins subject to eustatic sea-level change. Using rates of sea-level change, sediment supply and fault slip reported from active rift basins, the evolution of deltas located in three contrasting structural settings is documented: (1) footwall-sourced deltas in high-subsidence locations near the centre of a fault segment; (2) deltas fed by large drainage catchments at fault tips; and (3) deltas sourced from drainage catchments on the hangingwall dip slope. Differences in the three-dimensional form and internal stratigraphy of the deltas result from variations in tilting of the hangingwall and the impact of border fault slip rates on accommodation development. Because subsidence rates near the centre of fault segments are greater than all but the fastest eustatic falls, footwall-sourced deltas lack sequence boundaries and are characterized by stacked highstand systems tracts. High subsidence and steep bathymetry adjacent to the fault result in limited progradation. In contrast, the lower subsidence rate settings of the fault-tip and hangingwall dip-slope deltas mean that they are subject to relative sea-level fall and associated fluvial incision and forced regression. Low gradients and tectonic tilting of the hangingwall influence the geometry of these deltas, with fault-tip deltas preferentially prograding axially along the fault, creating elongate delta lobes. In contrast, broad, sheet-like delta lobes characterize the hangingwall dip-slope deltas. The model results suggest that different systems tracts may be coeval over length scales of several kilometres and that key stratal surfaces defining and subdividing depositional sequences may only be of local extent. Furthermore, the results highlight pitfalls in sequence-stratigraphic interpretation and problems in interpreting controlling processes from the preserved stratigraphic product.

Keywords Deltas, normal faults, numerical modelling, rift basins, sea-level change, sequence stratigraphy.

INTRODUCTION

The growth of basin-bounding normal fault zones is recognized as a first-order control on the size and shape of rift basins (e.g. Anders & Schlische, 1994; Gawthorpe *et al.*, 1994), on their large-scale, vertical stratigraphic evolution (e.g. Prosser, 1993; Contreras *et al.*, 1997; Gupta *et al.*, 1999) and on the three-dimensional variability of syn-rift depositional sequences (e.g. Gawthorpe *et al.*, 1994; Howell & Flint, 1994; Gawthorpe & Leeder, 2000). However, there is still much debate regarding the main processes controlling stratal geometry and cyclicity within syn-rift successions, largely because of the difficulty in unequivocally differentiating tectonic signals from those associated with variations in sediment supply and/or base level (e.g. Dart *et al.*, 1994; Hardy *et al.*, 1994).

[1]Present address: BP Exploration, Compass Point, 79–87 Kingston Road, Staines, TW18 1DY, UK.

Studies aimed at investigating the controls on syn-rift stratigraphy in both active and ancient rift basins have focused on basin-margin, coarse-grained depositional systems such as alluvial fans and fan deltas (Colella, 1988; Dart *et al.*, 1994; Dorsey *et al.*, 1995, 1997; Gupta *et al.*, 1999; Soreghan *et al.*, 1999; Young *et al.*, 2000). Such studies suggest a wide range of controls on stratigraphy, including climate, eustatic sea level and fault slip. However, it is often not possible to trace particular stratigraphic intervals within fan or fan-delta successions along fault zones or around rift basins to document their variability unequivocally with respect to structural setting or sediment entry points. Furthermore, in many cases, dating landscape and/or stratigraphy is not of sufficiently high resolution to allow detailed comparison with known global or local processes such as eustatic sea-level change or climate.

Here, results are reported from a numerical forward model of linked subsidence, sediment supply, fan-delta deposition and eustatic sea-level variation for a marine rift basin. This study is a development of that of Hardy & Gawthorpe (1998), who focused on the effects of along-strike variation in slip rate and eustatic sea-level change on fan deltas deposited in the immediate hangingwall of a normal fault zone. Here, fluvial incision during relative sea-level fall (cf. Ritchie *et al.*, 1999), hangingwall deformation and spatial variations in sediment supply associated with transverse drainage catchments developed on the footwall scarp and hangingwall dip slope are included. Using rates of processes reported from studies of active extensional basins, this model is used to investigate the three-dimensional development of syn-rift depositional sequences in different structural settings within rift basins, and the variability of key stratal surfaces, such as sequence boundaries and marine flooding surfaces, and facies stacking patterns.

THREE-DIMENSIONAL NUMERICAL MODELLING OF TECTONICS AND SEDIMENTATION

The specific aim of this study is to investigate the effect of relative sea-level change, sediment supply and basin physiography on fan-delta stratigraphy in marine half-graben basins. The modelling approach used is cellular: a 12 km by 10 km area of the Earth's surface is represented by a grid of cells, with cell size appropriate to the scale of the processes being modelled, here

40 m × 40 m. The time evolution of the model consists of updating, at each time step, the height of the cells as a result of tectonic subsidence and erosional or depositional processes. Time steps are 20 years. For a more detailed mathematical and algorithmic description of the modelling approach, the reader is referred to Ritchie *et al.* (1999). The following sections describe the key elements of the modelling approach, namely: (1) half-graben structural geometry; (2) sediment sources and supply; and (3) sediment transport and fan delta deposition (Fig. 1A). In addition to these elements, sea-level change is simulated as a simplified fourth-order (100 ky) glacio-eustatic cycle with an amplitude of 120 m (Fig. 1B). The rates and scales of structural development and sediment supply used are within the range of
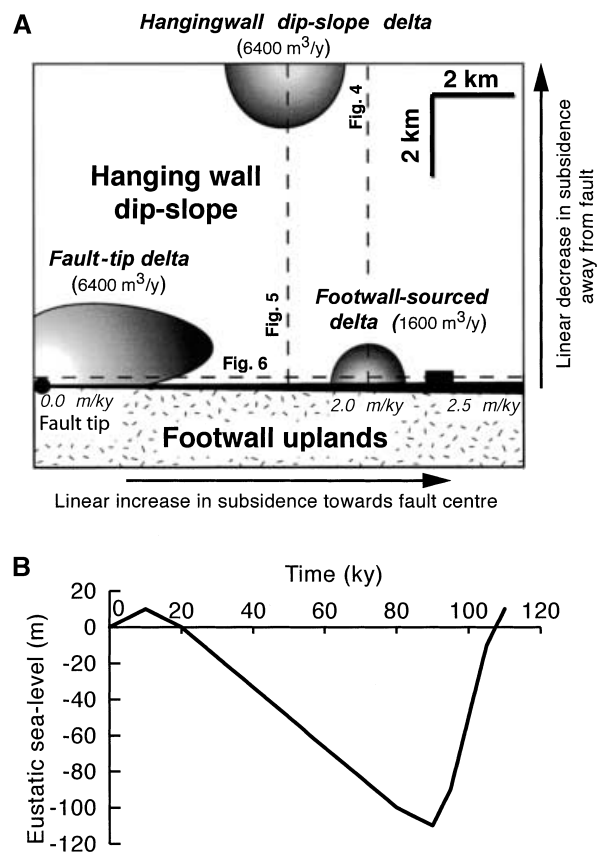
Fig. 1. (A) Schematic plan view of the three-dimensional numerical model of coarse-grained deltaic sedimentation in half-graben rift basins. The structure is based on half a fault segment (fault centre to tip), whereas sedimentation is simplified to three characteristic delta depositional systems sourced from: (1) footwall uplands; (2) fault tip; and (3) hangingwall dip slope. Fault slip rates and sediment supplies are based on active rift basins (see text for discussion). (B) Eustatic sea-level curve used in simulation, which is based on fourth-order glacio-eustatic sea-level changes.

rates reported from half-graben around the world (see Leeder, 1991; Leeder *et al.*, 1991; Dart *et al.*, 1994; Gawthorpe *et al.*, 1994; Hardy *et al.*, 1994), and sensitivity analysis of model results indicates that they are representative of half-graben of this scale and their interaction with eustatic sea-level variations.

Half-graben structural geometry

Structural studies of rift basins confirm that tilted fault blocks or half-graben are the fundamental basin element (Jackson, 1987; Leeder & Gawthorpe, 1987). Typically, half-graben are 5–20 km wide, on the order of 15–30 km long and are bounded on one side by major segmented normal fault zones (Fig. 2). The half-graben depocentres exhibit narrow, steep footwall scarps along the fault zone and gentler, broader hangingwall dip slopes. Furthermore, along-strike displacement gradients, with slip decreasing from fault centre to fault tip, lead to hangingwall topographic highs (commonly termed transverse anticlines; Schlische, 1995) at fault tips and depocentres associated with the area of highest displacement rates at fault centres (e.g. Gawthorpe *et al.*, 1994).

This characteristic half-graben basin geometry is modelled using a simple linear increase in hangingwall subsidence along a normal fault zone from 0 m ky^{-1} at the fault tip to 2·5 m ky^{-1} at the fault centre over a strike distance of 12 km (Fig. 1A). This is, in effect, half an idealized isolated fault segment and half-graben. Neither lateral propagation of the fault zone nor interaction with adjacent fault zones are considered in this model. The rates of subsidence used are within the range of rates reported from normal faults around the world (see Gawthorpe *et al.*, 1994; Hardy *et al.*, 1994). The fault is modelled as a simple vertical normal fault, separating a 2 km wide footwall upland above sea level, from a subsiding hangingwall basin (Fig. 1A). The horizontal component of fault displacement is not included (cf. Waltham & Hardy, 1995). Tilting of the hangingwall is modelled using a linear decrease in subsidence perpendicular to, and away from, the fault zone, reaching zero along the hangingwall edge of the model (Fig. 1A). The combination of fault-parallel displacement gradients and fault-perpendicular tilting results in hangingwall deformation that generates a three-dimensional, scoop-shaped depocentre typical of half-graben depocentres (Gawthorpe *et al.*, 1994; Schlische, 1995). In order to simulate deposition
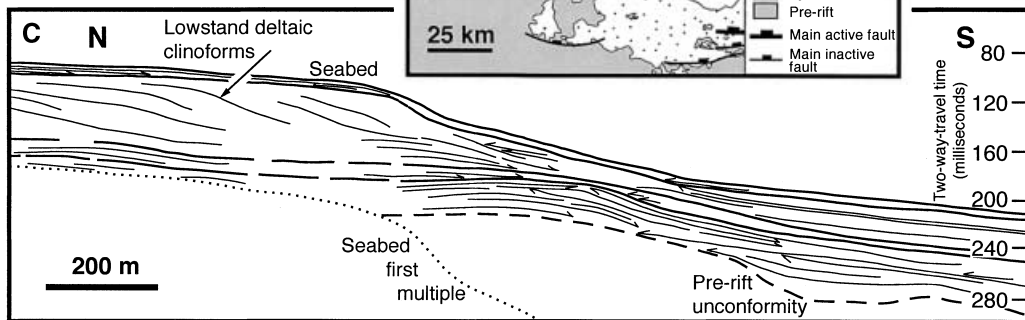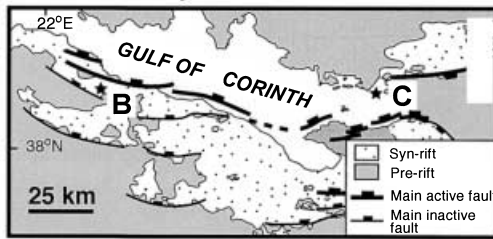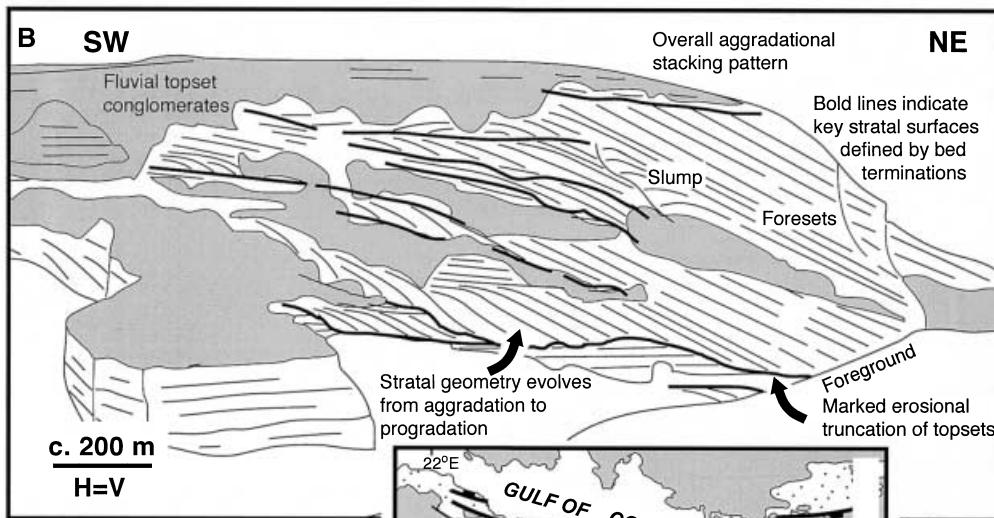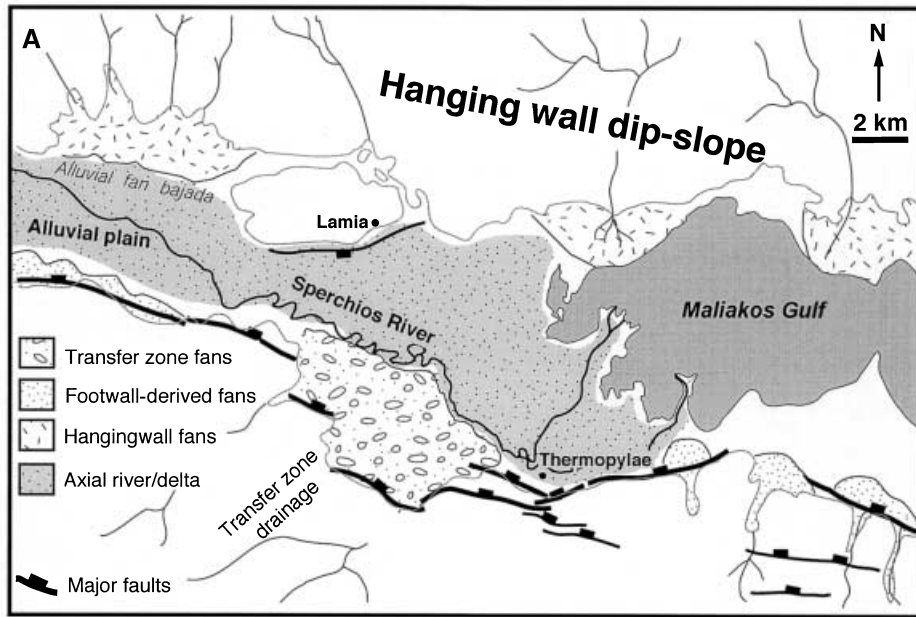
during the early stages of extension, the hangingwall starts with a pre-existing bathymetry of 50 m across the whole model; there are no pre-existing sediments or deltaic bodies. The footwall remains above sea level throughout the model run.

Sediment sources and supplies

Uplift and subsidence around normal fault zones results in pronounced asymmetry of rift basin topography that controls the development of transverse drainage catchments on footwall and hangingwall uplands (Fig. 2). Sediment supply from these drainage catchments acts as a primary control on the distribution of sedimentary environments and lithofacies (e.g. Leeder & Gawthorpe, 1987; Leeder, 1991; Leeder & Jackson, 1993; Gawthorpe & Leeder, 2000). These catchments supply sediment to fans and/or fan deltas deposited locally at the mouths of the catchments, or they combine and feed axial depositional systems (Fig. 2). A further control on drainage development is related to the segmented nature of the border fault zones, with fault offsets and transfer zones in the footwall commonly forming the locus of larger-than-average drainage basins (Fig. 2). This paper focuses on these structural controls on sediment supply, although additional factors such as bedrock lithology and antecedent drainage may also be locally important in controlling the spatial distribution of sediment supply in rift basins (e.g. Leeder *et al.*, 1991, 1998).

In order to simulate depositional systems sourced from the main structurally controlled drainage catchments, three fixed sediment entry points have been used (cf. Figs 1A and 2). Sediment derived from footwall catchments is represented by a single sediment entry point located on the fault scarp at a position where hangingwall subsidence is 2·0 m ky^{-1}. A further sediment entry point is located on the fault zone, at the fault tip, to reflect structurally controlled sediment supply at segment boundaries along the border fault zone. The third sediment entry point is located on the edge of the hangingwall dip slope to reflect hangingwall catchments. The rate of sediment supply has been set at 1600 m^3 year^{-1} for the sediment entry point located on the footwall scarp, and 6400 m^3 year^{-1} for both the fault-tip and the hangingwall entry points (Fig. 1A). These values are consistent with sediment yield data from similar structural settings in active extensional settings (e.g. Leeder *et al.*, 1991; Dart *et al.*, 1994).

At each of the three sediment entry points, the rate of sediment supply is kept constant

A

N

Hanging wall dip-slope

2 km

Alluvial fan bajada

Alluvial plain

Lamia•

Sperchios River

Maliakos Gulf

Transfer zone fans
Footwall-derived fans
Hangingwall fans
Axial river/delta

Thermopylae

Transfer zone drainage

Major faults

B **SW**

Overall aggradational
stacking pattern

NE

Fluvial topset
conglomerates

Bold lines indicate
key stratal surfaces
defined by bed
terminations

Slump

Foresets

Foreground

c. 200 m
H=V

Stratal geometry evolves
from aggradation to
progradation

Marked erosional
truncation of topsets

22°E

GULF OF CORINTH

B   C

38°N

25 km

Syn-rift
Pre-rift
Main active fault
Main inactive fault

C N

Lowstand deltaic
clinoforms

Seabed

S 80

Two-way-travel time
(milliseconds)

120

160

200

200 m

Seabed
first
multiple

Pre-rift
unconformity

240

280

throughout the model run. This assumption of constant sediment supply neglects likely spatial changes in sediment supply resulting from variation in bedrock lithology, uplift rates and slope gradients. Temporal variation in sediment supply over the 110 ky run caused by climate change is also not accounted for in the model (e.g. Leeder *et al.*, 1998; Collier *et al.*, 2000). These

Fig. 2. Examples of the characteristic structural geometry and depositional systems found in rift basins that were used to develop the numerical model (Fig. 1). (A) Sperchios basin, central Greece, illustrating half-graben form, segmented nature of border fault and main depositional systems (after Eliet & Gawthorpe, 1995). Note the large fans issuing from the major transfer zone along the border fault and the marked progradation of the axial fluvio-deltaic depositional system. (B) Line drawing of the Kerinitis footwall-derived fan delta, western Gulf of Corinth (see inset for location). Note the overall aggradational stacking pattern and the aggradational to progradational stratal geometry of the individual stratal units. The border fault that was active during deposition is located ≈1 km to the SW (after Dart *et al.*, 1994; Gawthorpe *et al.*, 1994). (C) Line drawing of seismic data showing a hangingwall dip-slope delta from the eastern Gulf of Corinth, Greece (see inset for location). Note the sheet-like, progradational geometry interpreted to result from deposition during eustatic sea-level fall and lowstand (after Collier *et al.*, 2000).

simplifications are made in order to allow investigation of the sensitivity of fan-delta stratigraphy solely as a result of variations in fault slip rate and hangingwall deformation.

Sediment transport and fan delta deposition

The modelling approach used here focuses specifically on the three-dimensional development of coarse-grained deltas that are typical of the depositional systems developed along rift basin margins (e.g. Leeder & Gawthorpe, 1987; Dart *et al.*, 1994; Dorsey *et al.*, 1995; Gupta *et al.*, 1999; Young *et al.*, 2000). The transport of coarse-grained sediment from a drainage basin outlet to a depositional basin, fluvial incision along sediment transport pathways and deltaic deposition are all addressed. A full discussion of the development of this three-dimensional modelling approach and its algorithmic details is given by Ritchie *et al.* (1999).

To represent sediment transport along fluvial distributary channels, sediment is transported from an input cell (a drainage basin outlet) to open water (a marine basin), using a combination of a random walk and a steepest descent algorithm. Where the topographic surface is subhorizontal (< 0·5°; see Ritchie *et al.*, 1999), the random walk algorithm is used. For inclined surfaces (> 0·5°), the steepest descent algorithm is applied. In this way, the fundamental gravitational control on downslope sediment transport is addressed. Upon arrival at open water, the transported sediment is deposited in the available

accommodation (see Hardy & Gawthorpe, 1998). A non-linear (threshold) three-dimensional diffusion equation is used to model downslope sediment movement (slumping, avalanching, etc.) when delta foreset slopes exceed a critical slope angle of 10°, a foreset angle of repose commonly reported for coarse-grained deltas (e.g. Nemec, 1990). Modification of the delta front by tide and wave processes is not modelled.

A key element in understanding the stratigraphic evolution of the deltas is modelling of channel incision associated with exposure of the topset–foreset transition during relative base-level fall. Although there are a number of factors that control fluvial incision (e.g. stream power, bedrock lithology, rate of sea-level fall, etc.), a first-order control on channel incision (knick-point migration) appears to be slope change (e.g. Leeder & Stewart, 1996). In the model, discharge variations along channels are not taken into account and, thus, channel incision is modelled as a simple advective process that is dependent only on local slope and an advective erosion rate constant. Incision occurs along transport pathways where their slope is greater than an equilibrium slope (representing the equilibrium profile of a fluvial channel). In this way, channels are initiated and cut back headwards from slope breaks above this equilibrium value (e.g. exposed shelf breaks during relative sea-level fall) in a manner similar to natural channels (Posamentier *et al.*, 1992; Wood *et al.*, 1993; Leeder & Stewart, 1996). When the sediment package reaches the shoreline, it thus includes the initial sediment supply and any eroded material collected on its transport path (see Ritchie *et al.*, 1999).

In the model results discussed here, it is assumed that the distributary channels have a grade of 1·0°, typical of coarse-grained fan-delta systems (e.g. Postma, 1990). When these distributary channels are out of grade, erosion is modelled using an advective erosion rate constant of 0·3 m ky^{-1}. Rates of channel incision and growth are poorly known and are likely to be controlled by many factors. In particular, the value of the advective erosion rate constant is not simple to relate to either bedrock or climate. Broadly, however, a high value represents easily erodable bedrock or high discharge, whereas a low value reflects resistant bedrock or low discharge. The importance of variation in the advective rate constant and its effect on delta morphology has been investigated by Ritchie *et al.* (1999), and the value used here lies in the middle of the range of

values investigated by Ritchie *et al.* (1999). In the subaqueous realm, a diffusion coefficient of 10 m^2 year^{-1} has been used to model slope failure where slopes build above our critical slope gradient of 10°.

STRATIGRAPHIC EVOLUTION OF HALF-GRABEN DEPOSITONAL SYSTEMS

Figure 3 illustrates the main stages in the morphological evolution of the model half-graben and
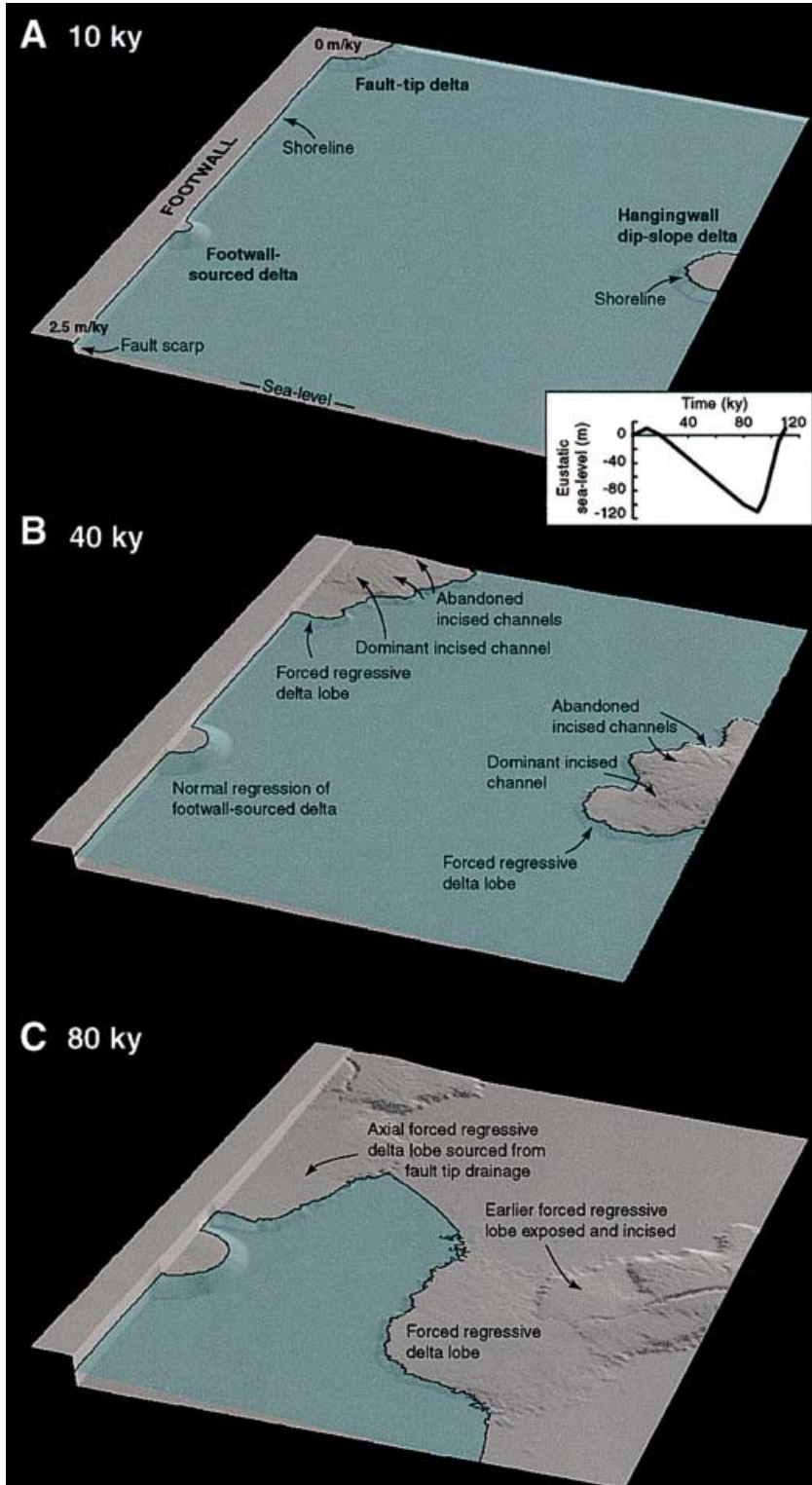
Fig. 3. (A–F) Selected three-dimensional oblique views across the model documenting the morphological development of the three delta systems in response to fault slip and eustatic sea-level change. Fault centre is located at bottom left, and fault tip at top left. The fault is 12 km long, and the fault perpendicular length of the model is 10 km, vertical exaggeration is ×3 (for details, see Fig. 1). The blue surface represents the sea surface, with the shoreline highlighted in black, so that grey areas on the top surface of the model are above sea level. Lighting is from the top, fault-tip side of the model. See text for discussion.

the three component fan deltas during the simplified glacio-eustatic sea-level cycle shown in Fig. 1. After 10 ky (Fig. 3A), three small fan deltas have formed and are localized at the sediment entry points. Each delta has a subhorizontal delta top and an arcuate shoreline separating the delta top from the delta slope. All the deltas show components of both aggradation and progradation and have a basinward-climbing shoreline trajectory, characteristics of normal regression during
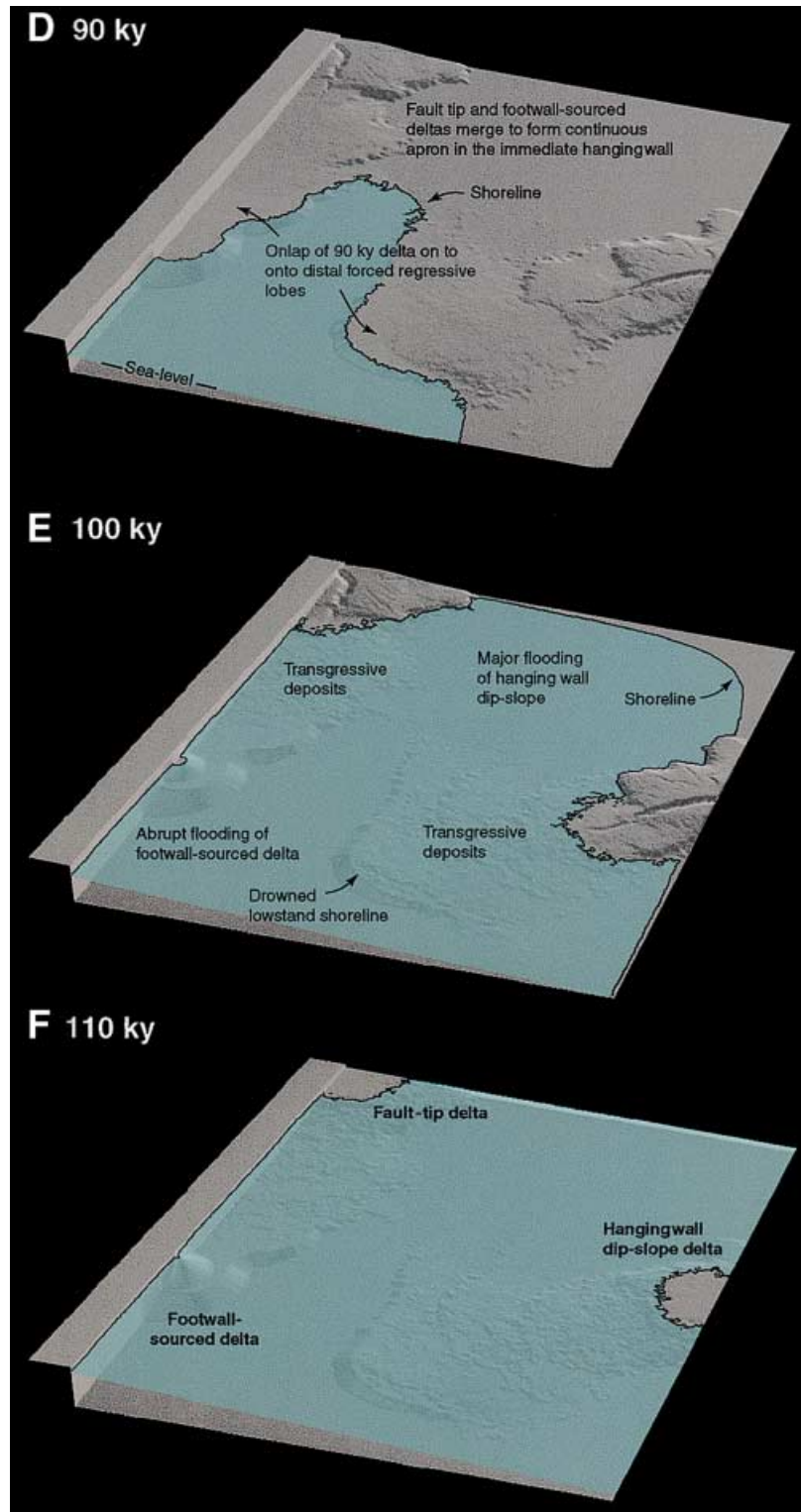

Fig. 3. (Continued).

relative sea-level rise (e.g. Posamentier & Vail, 1988). The low sediment supply and high subsidence rate of the footwall-sourced delta result in a cone-shaped aggradational delta that has a narrow, ≈100 m wide delta top and high foresets (≈ 250 m high) (Figs 3A and 4A). In contrast, the fault-tip and hangingwall deltas are more progradational, extending ≈ 950 and ≈ 750 m into the basin from their sediment entry points respectively (cf. Figs 4A, 5A and 6A).

From 10 to 90 ky, the background (eustatic) sea-level falls by 120 m, with a maximum rate of fall of 2 m ky^{-1} attained between 20 and 80 ky. It is

during the period of eustatic fall that major variations in morphology and internal geometry develop between the three deltas (Fig. 3B–D). During the initial stages of eustatic fall between 10 and 20 ky, the deltas maintained a similar arcuate morphology to that developed at eustatic highstand, and deposition occurred as a continuous fringe along the delta fronts. The main difference at this early stage of eustatic fall is in the amount of progradation. By 20 ky, the footwall delta has prograded up to 250 m from the fault scarp, whereas the fault-tip and hangingwall dip-slope deltas have prograded ≈ 1500 m and ≈ 1100 m respectively.
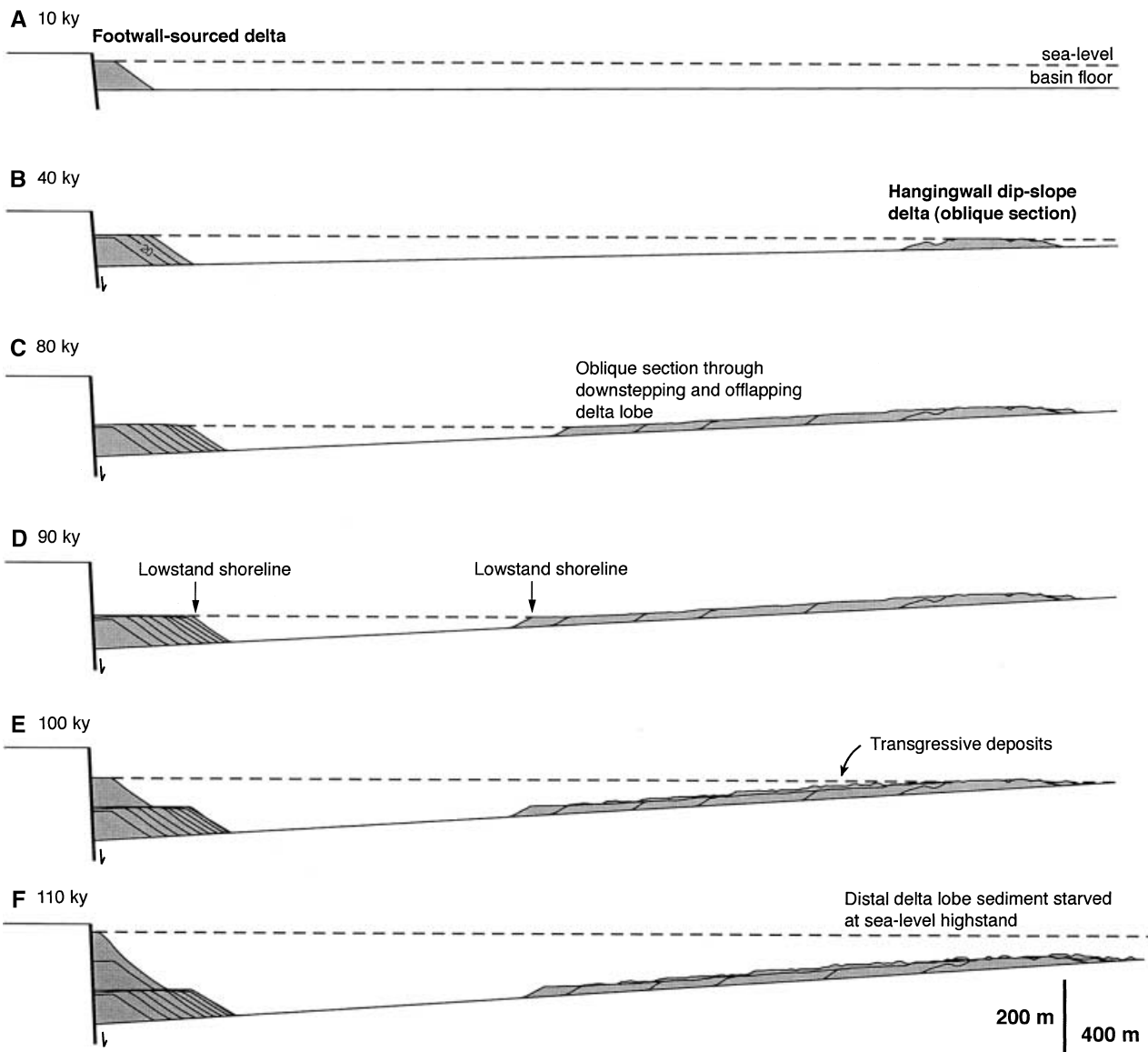
Fig. 4. Cross-sectional view of the model showing the evolution of stratal geometry. (A–F) The stages are illustrated in Fig. 3, and the section is located through the input point for the footwall-sourced delta and is perpendicular to the fault (see Fig. 1). Note vertical exaggeration.
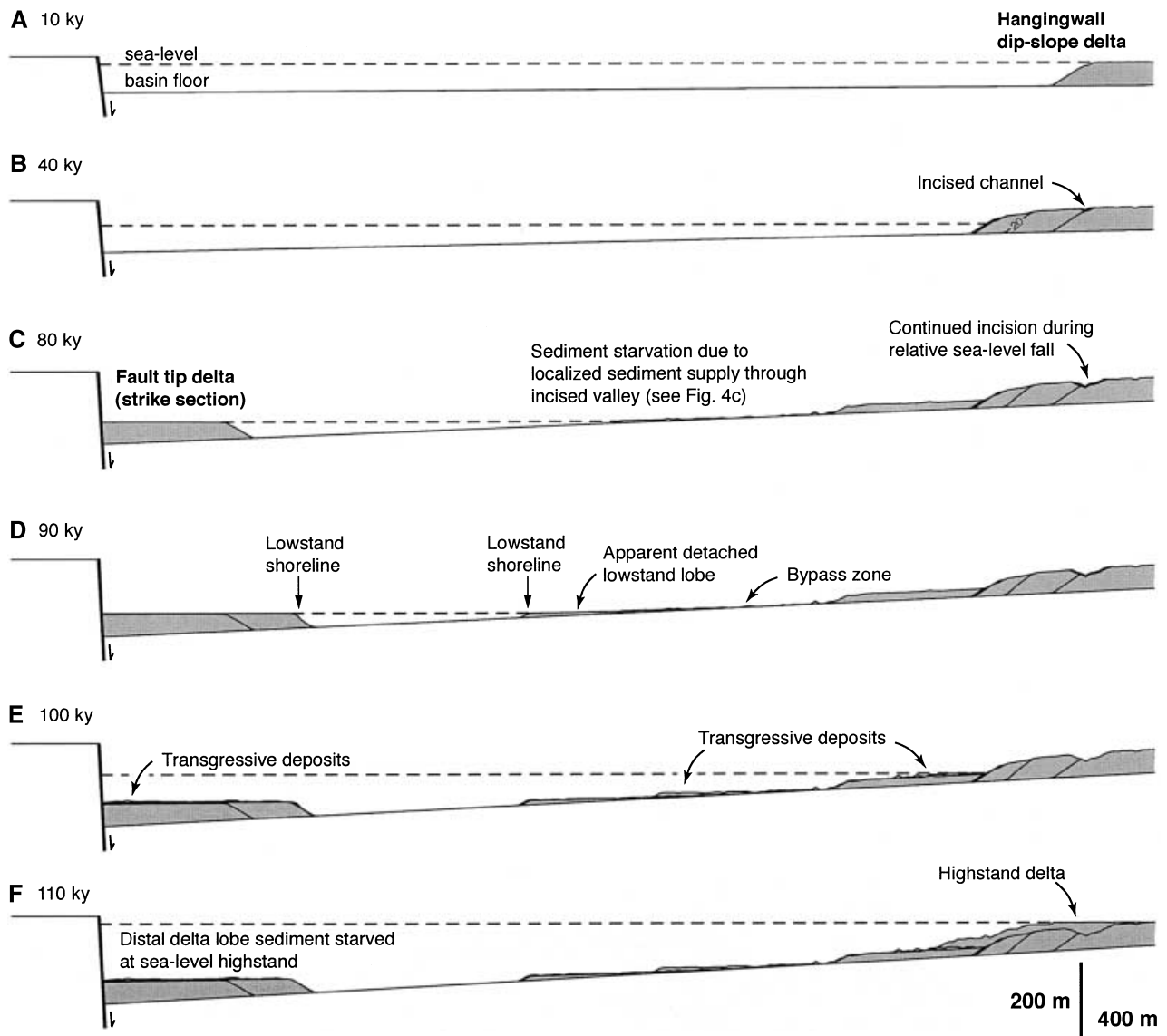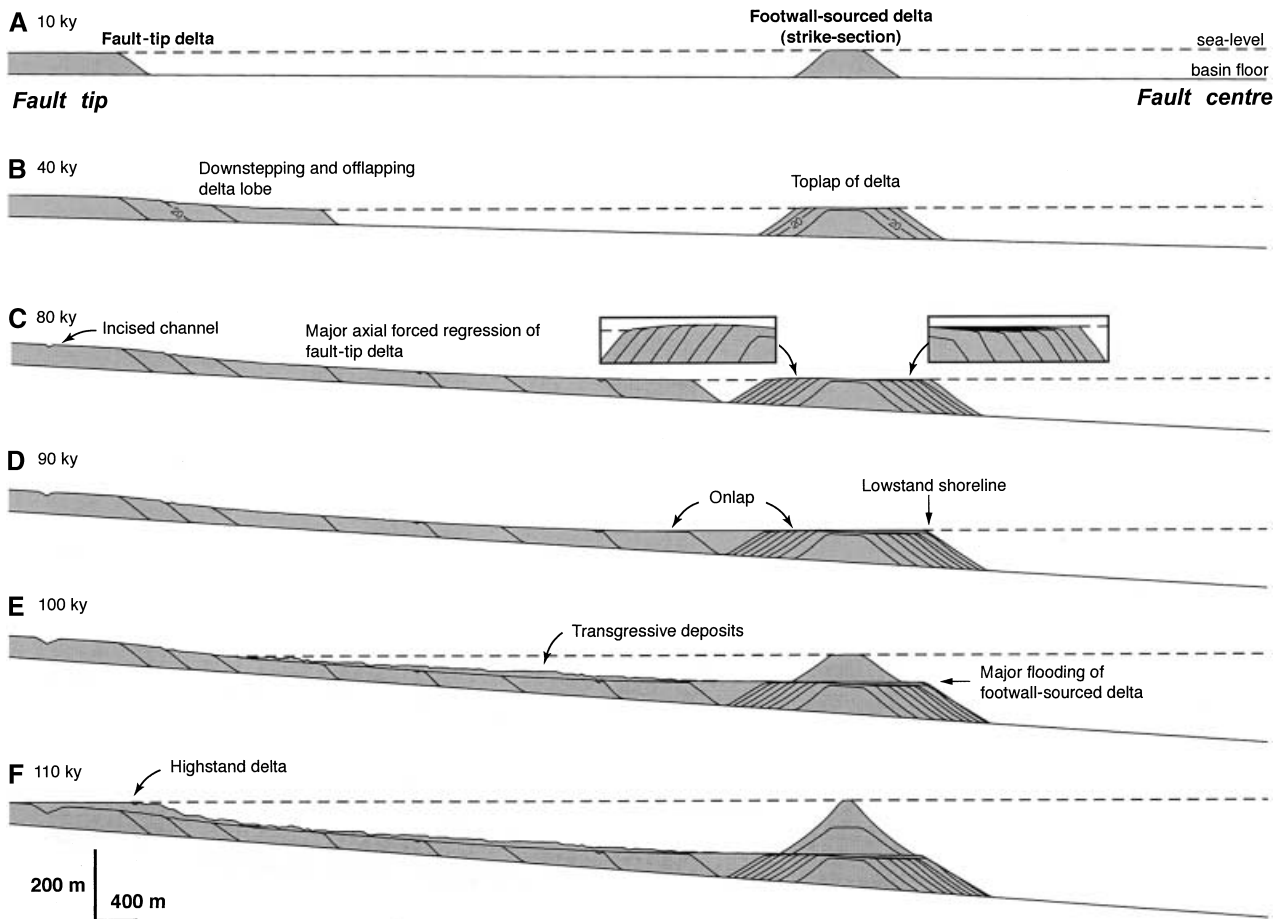
Fig. 5. Cross-sectional view of the model showing the evolution of stratal geometry. (A–F) The stages are illustrated in Fig. 3, and the section is located through the input point for the hangingwall dip-slope delta and is perpendicular to the fault (see Fig. 1). Note vertical exaggeration.

By 40 ky into the model run, eustatic sea level has fallen by 50 m, and marked variations in the morphology and internal geometry of the three deltas are apparent (Fig. 3B). The footwall-sourced delta still maintains the arcuate morphology developed during eustatic rise and early fall, but evolves into a progradational geometry with the shoreline extending up to 450 m from the fault (Figs 3B and 4B). The delta has a flat delta top with no evidence of offlap or incision. In contrast, both fault-tip and hangingwall dip-slope deltas have become incised by 40 ky, and the shoreline has developed a complex lobate form with distinct delta lobes 500–1750 m wide, separated by

embayments 200–600 m deep (Fig. 3B). The delta top of both fault-tip and hangingwall dip-slope deltas dips seawards, associated with offlap and downstepping of the deltaic lobes (Figs 5B and 6B). These features are characteristic of shallow-marine and deltaic deposition resulting from forced regression during relative sea-level fall (e.g. Plint, 1988; Hunt & Tucker, 1992; Posamentier et al., 1992).

The incised channels developed by headward erosion from the shoreline shortly after the onset of relative sea-level fall at 10 ky, and numerous incised channels developed initially. By 40 ky, however, most of the earlier formed incised

Fig. 6. Cross-sectional view of the model showing the evolution of stratal geometry. (A–F) The stages are illustrated in Fig. 3, and the section is parallel to the fault and located in the immediate hangingwall (see Fig. 1); it is viewed looking into the hangingwall. Note vertical exaggeration.

channels have been abandoned, and sediment transport has become localized through a small number of incised channels that are preferentially developed in the direction of tectonic tilt. These major incised channels supply sediment to point-sourced delta lobes at their mouths (Fig. 3B; cf. Ritchie *et al.*, 1999). For example, incision in the fault-tip delta is dominantly axial with respect to the fault, leading to the development of an offlapping delta lobe that downsteps parallel to the fault in the direction of increasing displacement (Figs 3B and 6B). By 40 ky, this delta lobe has prograded axially 3000 m from the sediment entry point.

In a similar way, incision on the hangingwall dip-slope delta becomes preferentially developed in the direction of tectonic tilt. One major incised valley, orientated in the direction of tilt, has developed by 40 ky and has captured flow that was previously going through many earlier formed incised channels (Fig. 3B and C). As a

result, deposition is localized at the mouth of the major incised channel as a 1750 m wide, down-stepping delta lobe that extends basinward by ≈ 1750 m from the sediment entry point (Fig. 3B). This prominent delta lobe progrades obliquely across the hangingwall dip slope, down the local tectonic tilt (Fig. 3B). Thus, the dip section through the sediment entry point of the hangingwall delta shows the exposed, incised and bypassed proximal delta top with virtually no deposition between 30 and 40 ky (Fig. 5B). In contrast, the dip section located 200 m along-strike towards the centre of the fault segment shows an oblique section through the mounded form of the 30–40 ky delta lobe deposited at the mouth of the major incised channel (Fig. 4B).

At the end of the period of maximum rate of eustatic sea-level fall at 80 ky, over half the hangingwall dip slope has become subaerially exposed (Fig. 3C). Overall, the morphology and internal geometry of the footwall-sourced delta is

similar to earlier stages in its development, and it has continued to prograde, the shoreline now reaching ≈ 780 m into the hangingwall from the fault (Figs 3C and 4C). The strike section through the footwall-sourced delta (Fig. 6C) illustrates the delicate balance between relative sea-level change and stratal geometry. Towards the fault tip, the strike section displays minor offlap and downstep between 20 and 80 ky (Fig. 6C). Here, the subsidence along the fault is slightly less than the rate of eustatic fall (2 m ky^{-1}), creating a minor relative sea-level fall. In contrast, towards the centre of the fault segment, the equivalent deltaic wedges display progradation with minor aggradation, and a slightly rising shoreline trajectory. In this location, the subsidence rate is slightly greater than the rate of eustatic fall, resulting in a minor relative sea-level rise. In many ways, the pronounced sequence variability illustrated by the footwall-sourced delta during the eustatic fall is a microcosm of the variability within the half-graben as a whole.

By 80 ky, both the fault-tip and the hangingwall dip-slope deltas have undergone marked regression (Fig. 3C) and, landward of the 80 ky shoreline, the earlier formed downstepping deltaic wedges have become subaerially exposed and incised (Figs 3C, 5C and 6C). The geometry of the fault-tip delta has become markedly elongate, with the shoreline migrating some 3500 m parallel to the fault between 40 and 80 ky. The delta becomes progressively narrower, extending only 750–1000 m away from the fault as it progrades into progressively deeper water (Fig. 3C). In contrast, the hangingwall dip-slope delta has a more sheet-like, lobate form, the shoreline having migrated a maximum of 3500 m obliquely down the hangingwall dip slope between 40 and 80 ky, and formed a broad delta lobe ≈ 4600 m wide (Fig. 3C).

At the lowstand of eustatic sea level at 90 ky, all three deltas have reached their maximum point of regression (Fig. 3D). The delta sourced from the fault tip and the footwall-sourced delta have merged to form a continuous fringe of deposition in the immediate hangingwall of the fault zone (Fig. 3D). The delta top in all three deltas has a smooth and subhorizontal form immediately behind the 90 ky lowstand shoreline that contrasts with the incised, downstepping nature of the more proximal, exposed portion of the fault-tip and hangingwall dip-slope delta tops (cf. Fig. 3C and D). In cross-section, the smooth, subhorizontal portion of the delta top is associated with slight aggradation between 80 and

90 ky and onlap onto the 80 ky surface. This is best displayed in the strike section in the immediate hangingwall of the fault (Fig. 6D). Comparison of the amount of onlap and aggradation between the fault-tip and footwall-sourced deltas indicates that the amount of aggradation increases with increasing subsidence along the fault zone (Fig. 6D). Thus, although eustatic sea level was still falling between 80 and 90 ky, the lower rate of eustatic fall (compared with the rate between 20 and 80 ky) and the relatively high subsidence, basinal location of the shoreline of all three deltas between 80 and 90 ky, resulted in deposition under conditions of a relative sea-level rise.

The eustatic sea-level rise from 90 ky to the end of the model run at 110 ky produces a marked landward shift in shoreline position in all three deltas as the rate of relative sea-level rise outpaces sediment supply (Fig. 3E and F). In the footwall-sourced delta, the preceding delta top is abruptly drowned and is downlapped by the toes of a small conical delta deposited in the immediate hangingwall of the fault (Fig. 4E and F). During the eustatic rise, the fault-tip and hangingwall dip-slope deltas are characterized by a series of low-relief mounded deposits that retrograde back towards the sediment entry points (e.g. Figs 3E, 4E and 6E). These transgressive deposits are fed through, and infill, the incised valleys cut during the earlier phase of relative sea-level fall.

At the end of the model run at 110 ky (Fig. 3F), the fault-tip and hangingwall dip-slope deltas occupy similar positions to those attained during the initial highstand of eustatic sea level (i.e. at 10 ky; Fig. 3A). In cross-section, the two deltas have components of aggradation and progradation, and downlap onto the retrogradational deposits (Figs 4F and 6F). Thus, both deltas display characteristics of normal regression formed as a result of sediment supply outpacing relative sea-level rise. In contrast, the footwall-sourced delta at 110 ky has almost no topsets and is almost entirely a submarine cone building onto the 90 ky submerged delta top that is now ≈ 160 m below sea level (Figs 3F and 4F).

DISCUSSION OF MODEL RESULTS AND IMPLICATIONS FOR SEQUENCE DEVELOPMENT AND VARIABILITY

Although the results presented were generated for one numerical model with a specific set of parameters, they provide more general insights

into depositional sequence development and the three-dimensional variability of sequences and their component stratal units and key stratal surfaces. These results, and the general and specific conclusions drawn from them, are in agreement with other numerical and analogue studies of such systems (e.g. Contreras & Scholz, 2001; Heller *et al.*, 2001; Csato & Kendall, 2002).

The cross-sectional stratal geometries, together with the surfaces representing the three-dimensional morphology of the depositional systems at specific times during their evolution, are perhaps most akin to seismic stratigraphy, rather than higher resolution outcrop-based depositional sequence analysis based on detailed facies analysis. In this section, the differences between the three deltas developed in the model and their implications for sequence development and variability are discussed. Key issues that arise from the results are also compared with natural examples of deltas in half-graben basins.

External form of deltas

The model presented for an idealized half-graben rift basin indicates that local, fault-controlled tectonic subsidence has a major impact on the three-dimensional external form and internal stratal geometry of coarse-grained deltas. In terms of the three-dimensional external form of the deltas, major differences are apparent between the footwall-sourced, fault-tip and hangingwall dip-slope deltas because of the impact of border fault slip rates and local tectonic tilting on accommodation development and basin physiography.

The steep bathymetric gradients that develop along the fault scarp, particularly near the centre of the modelled fault segment, coupled with limited sediment supply from small footwall drainage catchments, lead to coarse-grained deltas that have a cone- or fan-shaped morphology and undergo limited progradation (in the model <1 km). Hangingwall dip-slope deltas, in comparison, build into shallow water, on account of the lower gradient of the hangingwall dip slope, and with low subsidence rates. The shallow water depths, together with relatively large sediment supplies from hangingwall catchments, generate deltas that have a broad sheet-like to lobate form (in this low-energy basin where no tide or wave effects are modelled). Low subsidence rates also make the deltas prone to eustatic sea-level fall, leading to pronounced forced regression. In the model presented here, the lowstand shoreline of the hangingwall dip-slope delta is located 5–6 km basinward of the sediment entry point.
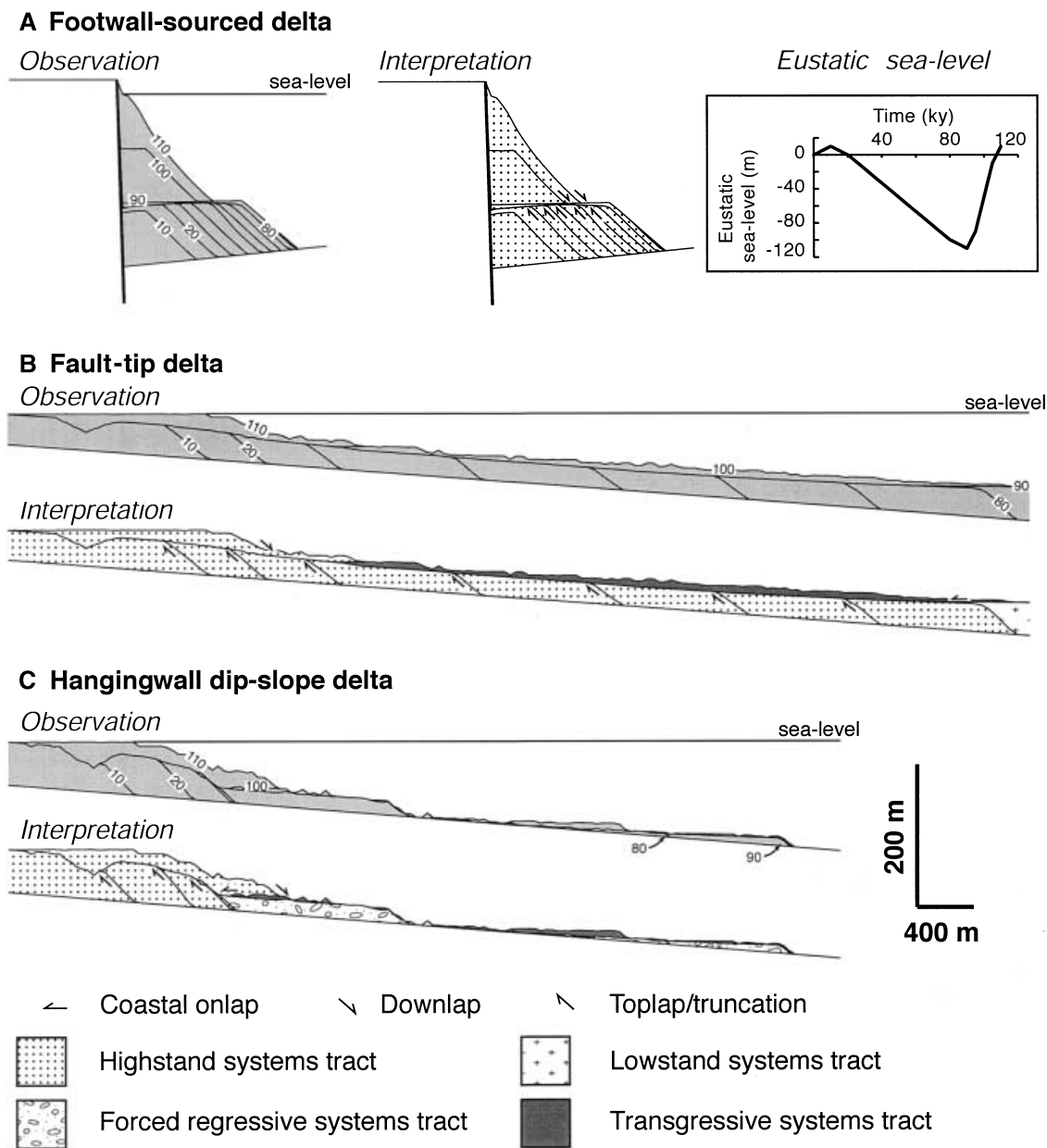
The fault-tip delta builds predominantly axially and develops an elongate external form as a result of tilting into, and parallel with, the fault. Low subsidence rates towards the fault tip make this type of delta prone to eustatic sea-level fall and, as a result, the fault-tip delta in the model undergoes marked regression, with the lowstand shoreline situated some 9 km along the fault from the sediment entry point. Despite the pronounced regression parallel to the fault, the shoreline only extends up to 1·5 km into the hangingwall and narrows progressively as it builds into deeper water towards the centre of the fault (e.g. Fig. 3C).

The morphological characteristics of the various modelled deltas are typical of natural examples from rift basins. For example, in the active Sperchios basin, Greece (Fig. 2; Eliet & Gawthorpe, 1995), the footwall-sourced, hangingwall dip-slope and axial deltas have similar planform morphology and areal extent to those in the numerical model presented here. In the Gulf of Corinth and Gulf of Patras half-graben, Greece, steep-gradient, cone- to fan-shaped fan deltas, with an area of 1–2 km², dominate the southern fault-bounded margin of the basins (e.g. Ferentinos *et al.*, 1988; Leeder *et al.*, 2002). In contrast, major hangingwall rivers feed broad, sheet-like deltas, such as the Evinos and Mornos deltas that have delta top areas of several tens of square kilometres (e.g. Piper *et al.*, 1990; Chronis *et al.*, 1991; Collier *et al.*, 2000).

Internal stratal geometry of deltas

Although there are gross similarities in the evolution of the three deltas, namely they all have an initial regressive phase followed by transgression and a final phase of limited regression, there are marked differences in their sequence stratigraphy (Fig. 7). Two key stratal surfaces can be recognized in the deltas based on stratal geometry, shoreline trajectory and stratal terminations. These are: (1) a transgressive surface, marked by onlap and a landward shift in the position of the shoreline that caps the initial phase of regression; and (2) a downlap surface (maximum flooding surface) that lies at the base of the final phase of limited regression (*sensu* Mitchum *et al.*, 1977; Posamentier & Vail, 1988).

In situations with low-gradient delta tops, low sediment supply and/or high rates of relative sea-level rise, such as in the footwall-sourced delta

A Footwall-sourced delta

Observation

Interpretation

Eustatic sea-level

B Fault-tip delta

Observation

Interpretation

C Hangingwall dip-slope delta

Observation

Interpretation

200 m

400 m

Coastal onlap ⟍ Downlap ⟍ Toplap/truncation

Highstand systems tract — Lowstand systems tract

Forced regressive systems tract — Transgressive systems tract

Fig. 7. Representative cross-sections showing the final stratigraphic product and sequence-stratigraphic interpretation for: (A) footwall-sourced delta; (B) fault-tip delta; and (C) hangingwall dip-slope delta. Numbered stratal surfaces are time in thousands of years, and the inset shows eustatic sea-level curve. Systems tract nomenclature follows that of Hunt & Tucker (1992) and Gawthorpe *et al.* (2000). See text for discussion.

near the centre of the fault segment, the transgressive surface and downlap surface are coincident, and there are no retrogradational deposits, i.e. no transgressive systems tract (Fig. 7A). In the fault-tip and hangingwall dip-slope deltas, low-relief mounded units retrograde up the exposed and seaward-dipping delta top and attest to deposition when the rate of accommodation development outpaced sediment supply (Fig. 7B and C). These deposits form a transgressive

systems tract and separate the transgressive surface at their base from the overlying downlap surface. Sediment deposited in these transgressive systems tract deposits is fed through, and progressively back-fills, the distal portions of incised channels.

Key stratal surfaces associated with relative sea-level fall, such as the sequence boundary and the basal surface of forced regression (e.g. Plint, 1988; Posamentier & Vail, 1988; Van Wagoner *et al.*,

1990; Hunt & Tucker, 1992; Posamentier *et al.*, 1992), are not equally developed in all three deltas. In high-subsidence settings, such as experienced by the footwall-sourced delta in the model, key stratal surfaces associated with sea-level fall are poorly developed, if at all (Fig. 7A). The footwall-sourced delta is located at the point where the rate of subsidence is equal to the fastest rate of eustatic fall (2 m ky^{-1} in the model). The delta essentially progrades, and the delta top is not incised during the phase of eustatic fall (Fig. 7A). The fault-tip side of the delta experiences slight relative fall, as the rate of eustatic fall is greater than the subsidence rate, whereas the fault-centre side of the delta experiences slight relative rise as subsidence rates are > 2 m ky^{-1}. This variation in relative sea level is expressed by subtle offlap towards the fault tip and slight aggradation of the topsets towards the fault centre (e.g. Fig. 6C). In practice, however, these subtleties would be difficult to identify, particularly on subsurface data (well logs or seismic), and a pragmatic interpretation would interpret the first regressive phase in the footwall-sourced delta to evolve from aggradational to progradational: a highstand systems tract. Thus, despite the background eustatic fall, the stratal geometry of the footwall-sourced delta would be interpreted in terms of deposition during relative sea-level rise.

Comparable stratal geometries are seen in natural examples from the Gulf of Corinth half-graben and the Suez rift (Dart *et al.*, 1994; Gawthorpe *et al.*, 1994; Gupta *et al.*, 1999). In the case of the Gulf of Corinth, ?Plio-Pleistocene fan deltas, now uplifted and incised in the footwall of the active normal fault zone, are dominated by aggradationally stacked stratal units, which evolve internally from aggradation to progradation and are bounded by major transgressive surfaces and/or downlap surfaces (e.g. the Kerinitis delta, Fig. 2B; Dart *et al.*, 1994; Gawthorpe *et al.*, 1994). Surfaces characterized by incision and across which there is a basinward shift in facies are rare.

In contrast to the footwall-sourced delta, the fault-tip and hangingwall dip-slope deltas show clear evidence for relative sea-level fall in the form of incised channels (Fig. 7B and C). Identification of the incised channels in proximal areas allows a sequence boundary to be picked at the base of the incised valleys and along associated interfluves. However, although there is clear evidence of incision and forced regression when the evolution of the system is visualized (Fig. 3), interpretation of relative sea-level fall from the final stratigraphic product is less clear. In the case of the modelled fault-tip delta, the main regressive deposits (0–90 ky) recorded in the final stratigraphy would be interpreted to reflect initial aggradation (0–10 ky), followed by progradation associated with toplap (10–80 ky) and, finally, onlap and aggradation/progradation (80–90 ky) (Fig. 7B). The subtle downstepping indicative of forced regression may be lost in the final product, partly because of the along-strike tilting of the delta topsets in the direction of regression (Fig. 7B). Thus, a pragmatic sequence-stratigraphic interpretation of the 0–80 ky stratigraphy is that it is a highstand systems tract formed during an initial relative sea-level rise and subsequent stillstand. Exposure and incision associated with relative sea-level fall then followed, before coastal onlap and the development of a lowstand wedge between 80 and 90 ky. This interpretation is clearly erroneous, misinterpreting the controls on the main phase of regression and the timing of relative sea-level fall.

In the hangingwall dip-slope delta (Fig. 7C), in addition to incision close to the sediment entry point, there is clear evidence of a downward shift in coastal onlap onto the 40 ky delta front and subsequent downstepping deltaic wedges up to 90 ky. Based on the two-dimensional cross-section in Fig. 7C, a practical sequence-stratigraphic interpretation would place all the 0–40 ky stratigraphy in a highstand systems tract, followed by the development of forced regressive and lowstand wedges until 90 ky. Interestingly, in the two-dimensional section through the sediment entry point of the hangingwall dip-slope delta, the 90 ky deltaic wedge appears to be a detached lowstand shoreline, separated from the updip delta by a zone of bypass (e.g. Fig. 5D). However, this is not a detached lowstand delta: in three dimensions, it is connected by a series of forced regressive delta wedges back to the initial highstand delta that formed at 10 ky (Fig. 3D).

Comparable stratal geometries to those developed in the modelled hangingwall dip-slope deltas are seen in natural examples from Greece along the hangingwall of the Gulfs of Patras and Corinth (e.g. Piper *et al.*, 1990; Collier *et al.*, 2000). For example, in the eastern Gulf of Corinth (Alkyonides Gulf), highly progradational, sheet- to wedge-shaped hangingwall dip-slope deltas are imaged in high-resolution shallow seismic data sets (Fig. 2C; Collier *et al.*, 2000). These deltas are interpreted to reflect deposition during late Quaternary eustatic sea-level falls when the gulf became an isolated lake

(Lake Corinth) because of a structural sill at its western end.

The sequence-stratigraphic analysis of the three modelled deltas has major implications for existing sequence-stratigraphic models and for interpreting the controls on stratigraphy. In particular, the modelling results raise questions regarding the chronostratigraphic significance of systems tracts when different systems tracts are developed contemporaneously within a basin over distance of several kilometres to tens of kilometres. Furthermore, the results highlight the problems in interpreting the controls on stratigraphy from the preserved stratigraphic product, particularly the timing and duration of relative sea-level fall, and the difficulty in deconvolving eustatic and tectonic components of relative sea-level change (e.g. Gawthorpe *et al.*, 1994; Hardy *et al.*, 1994; Csato & Kendall, 2002).

CONCLUSIONS

Despite the simplifications and assumptions used in the numerical model, the results presented here highlight the marked three-dimensional variability in depositional sequences that may develop in rift basins. In particular, the results indicate the importance of fault-related subsidence rates on relative sea-level change and basin physiography, and the impact that these factors have on sequence development. The results of the modelling study also have more general implications for sequence-stratigraphic interpretation of basin fills, highlighting the potential difficulties in correctly interpreting controls on stratigraphy in natural systems. In particular, this study indicates the problems in correctly identifying the stratigraphic products associated with relative sea-level fall and the practical problems in unequivocally relating the preserved stratigraphic product to the controlling processes.

The model results indicate that key stratal surfaces that define depositional sequences (e.g. the sequence boundary) or subdivide depositional sequences into component systems tracts (e.g. transgressive and maximum flooding surfaces) may be of limited spatial extent. In subsidence-dominated settings such as the hangingwall of rift basins, major marine flooding surfaces, such as the maximum flooding surface, are the most widespread, occurring in all three deltas in the model, and this surface is likely to have a distinctive lithological, biostratigraphic and seismic expression in natural systems. In contrast, key stratal surfaces associated with relative sea-level fall may be absent in certain structural settings and are often cryptic in others. For example, subaerial exposure and fluvial incision may be absent in the immediate hangingwall near the centre of fault segments, where subsidence rates may outpace all but the fastest eustatic falls. Even in settings where relative sea-level falls are pronounced, there are practical difficulties in correctly identifying the stratigraphy associated with relative sea-level falls. Recognizing the onset of relative sea-level fall from the stratigraphic product is particularly difficult.

Local subsidence rates also have a major impact on the development of systems tracts within depositional sequences. The marked spatial variations in relative sea-level change that result from local variations in fault-controlled subsidence lead to the development of different facies stacking patterns and stratal geometries in particular structural settings. This is most apparent during eustatic sea-level fall, when high subsidence rates adjacent to the centre of fault segments may lead to the continual creation of accommodation and the development of highstand systems tracts that are contemporaneous with forced regressive systems tracts in low subsidence rate locations. Variations in the development of the transgressive systems tract are also apparent around the modelled half-graben. Regions of low sediment supply, low coastal plain (delta top) gradients and high subsidence undergo abrupt transgression and lack retrogradational deposits of the transgressive systems tract. In contrast, in low subsidence rate settings that have higher sediment supplies and where transgression occurs over the seaward-dipping exposed top of downstepping forced regressive wedges, retrogradational deposits are developed and form a transgressive systems tract.

Although the model used here is a simplification of a complex natural system, and many processes are omitted (compaction, true drainage development in the footwall and climatic oscillations), it allows a better understanding of the three-dimensional stratigraphic evolution of half-graben basin fills. Furthermore, the results highlight pitfalls in sequence-stratigraphic interpretation and problems in interpreting controlling processes from the preserved stratigraphic product that are also applicable to other types of sedimentary basin.

ACKNOWLEDGEMENTS

REFERENCES

Anders, M.H. and Schlische, R.W. (1994) Overlapping faults, intrabasin highs and the growth of normal faults. *J. Geol.*, **102**, 165–179.

Chronis, G., Piper, D.J.W. and Anagnostou, C. (1991) Late Quaternary evolution of the Gulf of Patras, Greece: tectonism, deltaic sedimentation and sea-level change. *Mar. Geol.*, **97**, 191–209.

Colella, A. (1988) Pliocene-Holocene fan deltas of the Messina Strait. In: *Fan Deltas – Excursion Guidebook* (Ed. A. Colella), pp. 139–152. Universita della Calabria, Consenza, Italy.

Collier, R.E.L.I., Leeder, M.R., Trout, M., Ferentinos, G., Lyberis, E. and Papatheodorou, G. (2000) High sediment yields and cool, wet winters: test of last glacial palaeoclimates in the northern Mediterranean. *Geology*, **28**, 999–1002.

Contreras, J. and Scholz, C.H. (2001) Evolution of stratigraphic sequences in multisegmented continental rift basins: Comparison of computer models with the basins of the East African rift system. *AAPG Bull.*, **85**, 1565–1581.

Contreras, J., Scholz, C.H. and King, G.C.P. (1997) A model of rift basin evolution constrained by first-order stratigraphic observations. *J. Geophys. Res.*, **102**, 7673–7690.

Csato, I., and Kendall, C.G.StC. (2002) Modeling of stratigraphic architectural patterns in extensional settings – towards a conceptual model. *Comput. Geosci.*, **28**, 351–356.

Dart, C.J., Collier, R.E.L.I., Gawthorpe, R.L., Keller, J.V. and Nichols, G. (1994) Sequence stratigraphy of (?)Pliocene-Quaternary syn-rift, Gilbert-type deltas, northern Peloponnesos, Greece. *Mar. Petrol. Geol.*, **11**, 545–560.

Dorsey, R.J., Umhoefer, P.J. and Renne, P.R. (1995) Rapid subsidence and stacked Gilbert-type fan deltas, Pliocene Loreto basin, Baja California Sur, Mexico. *Sed. Geol.*, **98**, 181–204.

Dorsey, R.J., Umhoefer, P.J. and Falk, P.D. (1997) Earthquake clustering inferred from Pliocene Gilbert-type deltas in the Loreto basin, Baja California Sur, Mexico. *Sed. Geol.*, **25**, 679–682.

Eliet, P.P. and Gawthorpe, R.L. (1995) Drainage development and sediment supply within rift basins the Sperchios basin, central Greece. *J. Geol. Soc. London*, **152**, 883–893.

Ferentinos, G., Papatheodorou, G. and Collins, M.B. (1988) Sediment transport processes on an active submarine fault escarpment: Gulf of Corinth, Greece. *Mar. Geol.*, **83**, 43–61.

Gawthorpe, R.L. and Leeder, M.R. (2000) Tectono-sedimentary evolution of active extensional basins. *Basin Res.*, **12**, 195–218.

Gawthorpe, R.L., Fraser, A.J. and Collier, R.E.L. (1994) Sequence stratigraphy in active extensional basins: Implications for the interpretation of ancient basin fills. *Mar. Petrol. Geol.*, **11**, 642–658.

Gawthorpe, R.L., Sharp, I., Hall, M.T. and Dreyer, T. (2000) Forced regressions around propagating folds and faults. In: *Sedimentary Responses to Forced Regression* (Eds D.W. Hunt and R.L. Gawthorpe). *Geol. Soc. London Spec. Publ.*, 172, 177–193.

Gupta, S., Underhill, J.R., Sharp, I.R. and Gawthorpe, R.L. (1999) Role of fault interactions in controlling synrift sediment dispersal patterns: Miocene, Abu Alaqa Group, Suez Rift, Sinai, Egypt. *Basin Res.*, **11**, 167–189.

Hardy, S. and Gawthorpe, R.L. (1998) Effects of variations in fault slip rate on sequence stratigraphy in fan deltas: insights from numerical modelling. *Geology*, **26**, 911–914.

Hardy, S., Dart, C. and Waltham, D. (1994) Computer modelling of the influence of tectonics upon sequence architecture of coarse-grained fan deltas. *Mar. Petrol. Geol.*, **11**, 561–574.

Heller, P.L., Paola, C., Hwang, I.-G., John, B. and Steel, R. (2001) Geomorphology and sequence stratigraphy due to slow and rapid base-level changes in an experimental subsiding basin. *AAPG Bull.*, **85**, 817–838.

Howell, J.A. and Flint, S.S. (1994) A model for high resolution sequence stratigraphy within extensional basins. In: *High Resolution Sequence Stratigraphy: Innovations and Applications* (Eds J.A. Howell and J.F. Aitken), *Geol. Soc. London Spec. Publ.*, **104**, 129–137.

Hunt, D.W. and Tucker, M.E. (1992) Stranded parasequences and the forced regressive wedge systems tract: deposition during base level fall. *Sed. Geol.*, **81**, 1–9.

Jackson, J.A. (1987) Active normal faulting and crustal extension. In: *Continental Extensional Tectonics* (Eds M.P. Coward, J.F. Dewey and P.L. Hancock), *Geol. Soc. London Spec. Publ.*, **28**, 1–17.

Leeder, M.R. (1991) Denudation, vertical crustal movements and sedimentary basin fill. *Geol. Rundsch.*, **80**, 441–458.

Leeder, M.R. and Gawthorpe, R.L. (1987) Sedimentary models for extensional tilt-block/half-graben basins. In: *Continental Extensional Tectonics* (Eds M.P. Coward, J.F. Dewey and P.L. Hancock), *Geol. Soc. London Spec. Publ.*, **28**, 139–152.

Leeder, M.R. and Jackson, J.A. (1993) The interaction between normal faulting and drainage in active extensional basins, with examples from the western Unites States and central Greece. *Basin Res.*, **5**, 79–102.

Leeder, M.R. and Stewart, M.D. (1996) Fluvial incision and sequence stratigraphy: alluvial responses to relative sea-level fall and their detection in the geological record. In: *Sequence Stratigraphy in British Geology* (Eds S.P. Hesselbo and D.N. Parkinson), *Geol. Soc. London Spec. Publ.*, **103**, 25–39.

Leeder, M.R., Seger, M.J. and Stark, C.P. (1991) Sedimentation and tectonic geomorphology adjacent to major active and inactive normal faults, southern Greece. *J. Geol. Soc. London*, **148**, 331–344.

Leeder, M.R., Harris, T. and Kirkby, M.J. (1998) Sediment supply and climate change: implications for basin stratigraphy. *Basin Res.*, **10**, 7–18.

Leeder, M.R., Collier, R.E.L.I., Adul Aziz, L.H., Trout, M., Ferentinos, G., Papatheodorou, G. and Lyberis, E. (2002) Tectono-sedimentary processes along an active marine/

lacustrine half-graben margin. Alkyonides Gulf, E. Gulf of Corinth, Greece. *Basin Res.*, **14**, 25–41.

Mitchum, R.M., Vail, P.R. and Thompson, S. (1977) Seismic stratigraphy and global changes of sea level, part 2: the depositional sequence as a basic unit for stratigraphic analysis. In: *Seismic Stratigraphy – Applications to Hydrocarbon Exploration* (Ed. C.E. Payton), *AAPG Mem.*, 26, 53–62.

Nemec, W. (1990) Aspects of sediment movement on steep delta slopes. *Spec. Publ. Int. Assoc. Sedimentol.*, **10**, 29–73.

Piper, D.J.W., Stamatopoulos, L., Poulimenos, G., Doutsos, T. and Kontopoulos, N. (1990) Quaternary history of the Gulfs of Patras and Corinth, Greece. *Z. Geomorphol.*, **34**, 451–458.

Plint, A.G. (1988) Sharp-based shoreface sequences and 'off-shore bars' in the Cardium formation of Alberta; their relationship to relative changes in sea level. In: *Sea-Level Changes: an Integrated Approach* (Eds C.K. Wilgus, B.J. Hastings, H.W. Posamentier, J.C. Van Wagoner, C.A. Ross and C.G.StC. Kendall), *SEPM Spec. Publ.*, **42**, 357–370.

Posamentier, H.W. and Vail, P.R. (1988) Eustatic controls on clastic deposition II: sequence and systems tracts models. In: *Sea-Level Changes: an Integrated Approach* (Eds C.K. Wilgus, B.J. Hastings, H.W. Posamentier, J.C. Van Wagoner, C.A. Ross and C.G.StC. Kendall), *SEPM Spec. Publ.*, **42**, 126–154.

Posamentier, H.W., Allen, G.P. and James, D.P. (1992) High resolution sequence stratigraphy – the East Coulee delta, Alberta. *J. Sed. Petrol.*, **62**, 310–317.

Postma, G. (1990) Depositional architecture and facies of river and fan deltas: a synthesis. In: *Coarse-Grained Deltas* (Eds A. Colella and D.B. Prior), *Int. Assoc. Sedimentol. Spec. Publ.*, **10**, 13–27.

Prosser, S. (1993) Rift-related depositional systems and their seismic expression. In: *Tectonics and Seismic Sequence Stratigraphy* (Eds G.D. Williams and A. Dobbs), *Geol. Soc. London Spec. Publ.*, **71**, 35–66.

Ritchie, B., Hardy, S. and Gawthorpe, R.L. (1999) Three-dimensional modelling of coarse-grained clastic deposition in sedimentary basins. *J. Geophys. Res.*, **104**, 17759–17780.

Schlische, R.W. (1995) Geometry and Origin of Fault-Related Folds in Extensional Settings. *AAPG Bull.*, **79**, 1661–1678.

Soreghan, M.J., Scholz, C.A. and Wells, J.T. (1999) Coarse-grained, deep-water sedimentation along a border fault margin of Lake Malawi, Africa: seismic stratigraphic analysis. *J. Sed. Res.*, **69**, 832–846.

Van Wagoner, J.C., Mitchum, R.M., Campion, K.M. and Rahmanian, V.D. (1990) Siliciclastic sequence stratigraphy in well logs, core and outcrops. *AAPG Methods in Exploration Series*, **7**, 55 pp.

Waltham, D. and Hardy, S. (1995) The velocity description of deformation. Paper 1: Theory. *Mar. Petrol. Geol.*, **12**, 153–163.

Wood, L.S., Ethridge, F.G. and Schumm, S.A. (1993) The effects of rate of base level fluctuation on coastal-plain, shelf and slope depositional systems: an experimental approach. In: *Sequence Stratigraphy and Facies Associations* (Eds H.W. Posamentier, C.P. Summerhayes, B.U. Haq and G.P. Allen), *Int. Assoc. Sedimentol. Spec. Publ.*, 18, 43–53.

Young, M.J., Gawthorpe, R.L. and Sharp, I.R. (2000) Sedimentology and sequence stratigraphy of a transfer zone coarse-grained delta: Miocene Suez rift. Egypt. *Sedimentology*, **47**, 1081–1104.